



# Estimation of plate elastic moduli through vibration testing

Julien Caillet, Jean Claude Carmona, Daniel Mazzoni

## ► To cite this version:

Julien Caillet, Jean Claude Carmona, Daniel Mazzoni. Estimation of plate elastic moduli through vibration testing. *Applied Acoustics*, 2006, pp.334-349. 10.1016/j.apacoust.2006.01.011 . hal-01084749

**HAL Id: hal-01084749**

**<https://hal.science/hal-01084749>**

Submitted on 20 Nov 2014

**HAL** is a multi-disciplinary open access archive for the deposit and dissemination of scientific research documents, whether they are published or not. The documents may come from teaching and research institutions in France or abroad, or from public or private research centers.

L'archive ouverte pluridisciplinaire **HAL**, est destinée au dépôt et à la diffusion de documents scientifiques de niveau recherche, publiés ou non, émanant des établissements d'enseignement et de recherche français ou étrangers, des laboratoires publics ou privés.

# Estimation of plate elastic moduli through vibration testing <sup>☆</sup>

Julien Caillet <sup>a</sup>, Jean Claude Carmona <sup>a,\*</sup>, Daniel Mazzoni <sup>b</sup>

<sup>a</sup> *Laboratoire des Sciences de l'Information et des Systèmes, UMR CNRS 6168,  
Ecole Supérieure d'Ingénieurs de Marseille, 13451 Marseille Cedex 20, France*

<sup>b</sup> *Laboratoire des Mécanique et d'Acoustique, UPR CNRS 751, Ecole Supérieure d'Ingénieurs de Marseille,  
13451 Marseille Cedex 20, France*

Received 7 March 2005; received in revised form 24 January 2006; accepted 26 January 2006

Available online 27 April 2006

---

## Abstract

This paper considers the identification problem for 2D-structures by comparing a modal method with a new method based on the estimation of the dispersion equation in  $k$ -space. Both methods are validated by numerical simulation and by measurements based on an acoustic holography experiment.

© 2006 Elsevier Ltd. All rights reserved.

**Keywords:** Identification; Near-field acoustic holography; Dispersion equation; Elastic constants

---

## 1. Introduction

This paper is concerned with the general problem of acoustic comfort in air transportation with a special emphasis on aircraft and helicopter cabins. The results presented in this paper address both the diagnosis and modelling problems. Diagnosis is achieved by near-field acoustic holography techniques (NAH for short). NAH has been used to measure the vibro-acoustic fields (sound pressure, vibration velocity, sound intensity) on all the inner panels of a helicopter cabin. The experiment and the measure collection process

---

<sup>☆</sup> This work was supported by Eurocopter Inc.

\* Corresponding author. Tel.: +33 491 054 598; fax: +33 491 054 339.

E-mail address: [jean-claude.carmona@egim-mrs.fr](mailto:jean-claude.carmona@egim-mrs.fr) (J.C. Carmona).

are described in [1]. Our main interest in NAH here is to provide a measurement tool giving access to the 2D-vibration field without contact with these panels. Moreover, it is important to stress that one of the other advantages of NAH as compared to measurement techniques such as optical interferometry or laser vibrometry, is its low sensibility with respect to noisy data, and this feature is crucial for helicopter in-flight measurements.

In the present paper, the structures so obtained are used to model the vibrations and the acoustic radiations of the different cabin panels. Modelling cabin noise requires the identification of the mechanical properties of the radiating structures. The latter are generally made of stiffened composite panels, and the measurement of their elasticity constant is rather delicate. Therefore, we searched for an equivalent model based on the definition of an equivalent orthotropic plate for these complex structures, and we used “in situ” measurements to achieve this goal. To be specific, we developed this strategy from measurements made on a particular set of plates. However, the reader should easily convince herself that no significant loss of generality ensues, as the methods presented here can be applied to more complex cases. In fact, our objective was not to solve the direct plate vibration problem. Our main motivation was to use the plate vibration equations to validate the methods developed here, shooting for an estimate of the plate elastic moduli.

At low frequencies, the behavior of these structures is mostly modal driven: the vibrations can be described by the sum of the mode shapes of the structure. In this regime, a modal identification approach is proposed. At medium or high frequencies where the modal density becomes very important, this modal approach becomes inefficient. We provide a propagative description of the dynamics. Wave propagation parameters are identified, most notably the elastic wave numbers appearing in the dispersion equation.

Modelling the dynamic response of an orthotropic plate is a challenging problem which has been widely studied in the recent past. One of the first method used to tackle this problem was proposed by Aksu and Ali [2]. The authors used a finite difference method in order to compute the vibration response of a stiffened plate. In the same vein, Mukhopadhyay [3] proposed a different finite difference method to solve the vibration problem of an orthotropic plate. More recently, the finite element method was used to compute the dynamic response of orthotropic plates in [4,5]. A semi-analytical method was proposed by Dalaei and Kerr [6] in 1996 to compute the free vibrations of an orthotropic plate: the authors used an expansion of the solution in harmonics, recasting their approach in a Galerkin-like approach.

All the *direct problems* require the knowledge of the elastic constants of the orthotropic panel under investigation. In this sense, a given orthotropic panel is characterized by a set of four independent elastic constants [7]. Standard tests are available to determine these constants through mechanical probes [8]. However, these measurements are more delicate than for isotropic plates. As an alternative solution to the direct problem attempting to resolve the vibrations of an orthotropic plate, some authors have proposed *inverse methods* to identify the elastic constants of an orthotropic panel through vibration testing. Three approaches have been proposed. The first approach is based on measurements of the natural frequencies of the tested panel. An inverse identification technique is then used to obtain converged values of the elastic constants from the measured natural frequencies. This method requires the direct problem generally by Rayleigh–Ritz or Galerkin techniques is presented in [7,9] for example. The second approach presented by Grédiac and Paris [10], uses the same data that the first one, namely the measured natural frequencies of the panel, but works directly: neither initial values of the mechanical properties of the

plate, nor iterative computation are required. Nevertheless, these two methods are low frequency methods. The third method proposed by Berthaut and Ichchou [11] works at high frequencies. It is also a direct method in which the authors proposed to identify the parameters of the dispersion equation from vibrational velocity maps of the plate, measured by a laser vibro-meter, through projection of this measure on an inhomogeneous waves' base.

The method we propose in the present paper is direct, so it can be compared to [10]. It performs well at low frequencies. Also, it relies on the identification of a set of triplets  $(m, n, \omega_{mn})$  which represent the mode shapes  $W_{mn}$  and the natural frequencies of the structure. When compared to the approach used in [10], the main advantage of our method is its simplicity. Indeed [10] requires the computation of the variational principle for the measured mode shapes, forcing an integration over the measured mode shapes  $W_{mn}$ . In our approach, one merely needs to identify the triplets  $(m, n, \omega_{mn})$  corresponding to the mode shapes  $W_{mn}$  which represents a significant computational saving.

The paper is organized as follows: first a short preview of the main characteristics of the vibro-acoustic response of a specially orthotropic plate is given. The related equations are used in the numerical validation step presented later on. Then the principle of the identification of the elasticity constants of a special orthotropic plate is presented. It is based on different boundary conditions, such as simply supported and a clamped plates. In the following section, we validate this approach with the numerical analysis of a carbon–epoxy composite plate. Then, the dispersion equation of the identification is presented and compared to the modal approach according to the numerical model. Finally, we apply these methods to an experimental case study using near-field acoustic holography measures. We conclude with some perspectives for future work.

## 2. Vibro-acoustic response of a specially orthotropic panel

We use cartesian coordinates  $(0, \mathbf{x}, \mathbf{y}, \mathbf{z})$  in *free space*  $\mathbb{R}^3$ . A plane elastic rectangular panel  $\Sigma$  with length  $a$ , width  $b$ , and with a constant thickness  $h$ , is submitted to two different boundary conditions: simply supported boundary, or clamped boundary onto its boundary  $\partial\Sigma$ . We are interested in an industrial panel as one can find in an helicopter cabin. Since these panels are fairly rigid, we assume that the influence of the fluid on the vibro-acoustic response of the panel can be neglected. It is also assumed that the damping phenomenon can be neglected: this is a valid approximation since we consider stiffened steel panels or advanced composites such as carbon fiber-reinforced plastics.

In this section, we derive the time-harmonic system of equations governing the transverse vibrations of an “in vacuo” thin, specially orthotropic elastic plate.

Let us denote  $u(M)$  the transverse displacement of the plate  $\Sigma$  at the point  $M$  with coordinates  $(x, y)$ , submitted to an external time-harmonic force  $f(M)$ . The functions  $u$  and  $f$  are solutions of the following system of equations:

$$\begin{cases} D_1 \frac{\partial^4 U}{\partial x^4} + D_2 \frac{\partial^4 U}{\partial y^4} + 2(D_{12} + 2D_{66}) \frac{\partial^4 U}{\partial x^2 \partial y^2} - m\omega^2 U = -F & \forall M \in \Sigma \quad (\text{a}) \\ \text{Boundary conditions for } U \text{ onto } \partial\Sigma & (\text{b}) \end{cases} \quad (1)$$

where  $m$  denotes the mass of the plate per unit of surface,  $D_1$ ,  $D_2$  and  $D_{12}$  are the bending stiffness factors,  $D_{66}$  is the torsional stiffness which depends upon the transverse Young's moduli  $E_1$  and  $E_2$ , the shear-modulus  $G_{12}$  and the major and minor Poisson ratios  $\nu_{12}$  and  $\nu_{21}$  as explained for example, in [5,7,12]:

$$D_1 = \frac{E_1 h^3}{12(1 - \nu_{12}\nu_{21})}, \quad D_2 = \frac{E_2 h^3}{12(1 - \nu_{12}\nu_{21})} \quad (2)$$

In the sequel, we denote by  $D_3$  the following real number:

$$D_3 = D_{12} + 2D_{66} = \nu_{12}D_2 + \frac{G_{12}h^3}{6}, \quad \nu_{12}E_2 = \nu_{21}E_1 \quad (3)$$

Two boundary conditions (1b) are considered in the present paper:

Clamped plate:  $u = 0$  if  $M \in \partial\Sigma$ ,  $\partial_x u = 0$  if  $x \in \{0, a\}$  and  $\partial_y u = 0$  if  $y \in \{0, b\}$ .

Simply supported plate:  $u = 0$  if  $M \in \partial\Sigma$ ,  $\partial_x^2 u = 0$  if  $x \in \{0, a\}$  and  $\partial_y^2 u = 0$  if  $y \in \{0, b\}$ .

The identification method we propose here does not need to explicitly solve the above system of equations (1a,1b) for the displacement of the plate and its boundary conditions. This system is solved only for validation purposes: the numerical solutions of (1a,1b) for the bending stiffness of a given orthotropic plate  $D_1$ ,  $D_2$  and  $D_{12}$  and the torsional stiffness  $D_{66}$ , will give the vibrating responses of well-known specially orthotropic panels. These responses will then be introduced in our identification procedure. Finally, the identified bending stiffness factors will be compared to the computed ones.

The system (1a,1b) is solved numerically by using a high-order finite difference method to compute the bi-harmonic operator appearing in the plate equation (1a). The numerical study of the method used to solve the system (1a,1b) is presented in [13].

In the sequel, we examine the possibility of determining the elastic constants of a thin specially orthotropic plate by means of vibration testing and modal analysis.

### 3. Evaluation through low frequency modal analysis of elastic constants of a specially orthotropic plate

In this section a method is proposed to evaluate the transverse Young moduli  $E_1$ ,  $E_2$  and the in-plane shear modulus  $G_{12}$  of a specially orthotropic plate by vibration testing and modal analysis of a plate submitted to two different boundary conditions: simply supported boundary and clamped boundary.

#### 3.1. Identification on a simply supported plate

Consider a specially orthotropic simply supported rectangular plate of dimensions  $[a \times b]$ . Let us denote by  $W_{mn}$  the eigen-modes and  $\Omega_{mn}$  the eigen-angular frequencies of this plate. The functions  $W_{mn}$  and  $\Omega_{mn}$  solve the following system of equations:

$$\begin{cases} D_1 \frac{\partial^4 W_{mn}}{\partial x^4} + D_2 \frac{\partial^4 W_{mn}}{\partial y^4} + 2D_3 \frac{\partial^4 W_{mn}}{\partial x^2 \partial y^2} = m\Omega_{mn}^2 W_{mn} & (a) \\ W_{mn} = 0 & \text{if } x \in \{0, a\} \quad \text{or} \quad \text{if } y \in \{0, b\} & (b) \\ \partial_x^2 W_{mn} = 0 & \text{if } x \in \{0, a\} & (c) \\ \partial_y^2 W_{mn} = 0 & \text{if } y \in \{0, b\} & (d) \end{cases} \quad (4)$$

The eigen-modes  $W_{mn}$  and the eigen-angular frequencies  $\Omega_{mn}$  of a simply supported specially orthotropic plate of dimension  $[a \times b]$  are given by (see e.g. [12]):

$$W_{mn}(x, y) = \sin\left(\frac{m\pi}{a}x\right) \sin\left(\frac{n\pi}{b}y\right) \quad (5)$$

Let us denote by  $\xi$  and  $\eta$  the dual variables of  $x$  and  $y$  in the Fourier transform domain, as defined by:

$$\hat{W}_{mn}(\xi, \eta) = \int \int_{\mathbb{R}^2} W_{mn}(x, y) e^{i\xi x} e^{i\eta y} dx dy \quad (6)$$

The variables  $\xi$  and  $\eta$  are the wave numbers in the directions  $x$  and  $y$ . Taking the Fourier transform in space of (4a) leads to:

$$D_1 \xi^4 + D_2 \eta^4 + 2D_3 \xi^2 \eta^2 = m\Omega_{mn}^2 \quad (7)$$

When the space Fourier transform (6) is performed in an analytical way, then the expressions of the wave numbers  $\xi$  and  $\eta$  associated to the mode shape  $W_{mn}$  defined by the formula (5) become:

$$\xi = \xi_m = \frac{m\pi}{a}, \quad \eta = \eta_n = \frac{n\pi}{b} \quad (8)$$

The above expressions of  $\xi_m$  and  $\eta_n$  are introduced in Eq. (7) satisfied by the eigen-mode  $(\hat{W}_{mn}, \Omega_{mn})$ . This last equation when written in matrix form, gives:

$$\begin{bmatrix} \xi_i^4 & \eta_j^4 & 2\xi_i^2 \eta_j^2 \end{bmatrix} \begin{bmatrix} D_1 \\ D_2 \\ D_3 \end{bmatrix} = m\Omega_{ij}^2 \quad (9)$$

Suppose now that  $N$  couples of eigen-modes/eigen-frequencies of the simply-supported plate are known

$$\underbrace{\{(W_{ij}, \Omega_{ij}), \dots, (W_{kl}, \Omega_{kl})\}}_{N \text{ terms}} \quad (10)$$

The equations satisfied by each couple  $(W_{ij}, \Omega_{ij})$  define a set of  $N$  equations, with 3 unknowns: The flexural rigidities  $D_1$ ,  $D_2$ , and  $D_3$ :

$$\left\{ \begin{bmatrix} \xi_i^4 & \eta_j^4 & 2\xi_i^2 \eta_j^2 \\ \vdots & \vdots & \vdots \\ \xi_k^4 & \eta_l^4 & 2\xi_k^2 \eta_l^2 \end{bmatrix} \cdot \underbrace{\begin{bmatrix} D_1 \\ D_2 \\ D_3 \end{bmatrix}}_{[D]} = \underbrace{\begin{bmatrix} m\Omega_{ij}^2 \\ \vdots \\ m\Omega_{kl}^2 \end{bmatrix}}_{[B]} \right\} N \text{ lines} \quad (11)$$

When  $N$  is greater than 3, the system (11) can be solved by a least squares method. Let  $[A]^t$  denote the transposed matrix of the matrix  $[A]$ , and  $\{[A]^t \cdot [A]\}^{-1}$  the inverse of the matrix  $\{[A]^t \cdot [A]\}$ . The solution of the system (11) is given by:

$$[D] = \{[A]^t \cdot [A]\}^{-1} [A]^t \cdot [B] \quad (12)$$

The bending stiffness factor is given by the resolution of (12), and the Young and shear moduli of the plate come from Eqs. (2) and (3):

$$\begin{aligned}
E_1 &= \frac{12}{h^3} (D_1 - v_{12}^2 D_2) \\
E_2 &= \frac{D_2}{D_1} \frac{12}{h^3} (D_1 - v_{12}^2 D_2) \\
G_{12} &= \frac{6}{h^3} (D_3 - v_{12} D_2) \\
v_{21} &= \frac{v_{12} D_2}{D_1}
\end{aligned} \tag{13}$$

### 3.2. Identification on a clamped plate

The identification of the Young and the shear moduli of a clamped plate uses the results presented in [12,14]. For a clamped plate, the typical mode shapes are written as follows:

$$W_{mn}(x, y) = X_m(x) Y_n(y) \tag{14}$$

where  $X_m(x)$  and  $Y_n(y)$  are the mode shapes of the associated clamped beams of respective lengths  $a$  and  $b$ , so that:

$$X_m(x) = A_{1m} \sin(\alpha_m x) + A_{2m} \cos(\alpha_m x) + A_{3m} \sinh(\alpha_m x) + A_{4m} \cosh(\alpha_m x) \tag{15}$$

$$Y_n(y) = B_{1n} \sin(\beta_n y) + B_{2n} \cos(\beta_n y) + B_{3n} \sinh(\beta_n y) + B_{4n} \cosh(\beta_n y) \tag{16}$$

where the parameters  $A_{1m}, A_{2m}, A_{3m}, A_{4m}, B_{1n}, B_{2n}, B_{3n}, B_{4n}, \alpha_m$  and  $\beta_n$  proposed by [12] are:

$$\begin{aligned}
A_{1m} = -A_{3m} = 1, \quad A_{2m} = -A_{4m} &= \frac{\sinh(\alpha_m a) - \sin(\alpha_m a)}{\cos(\alpha_m a) - \cosh(\alpha_m a)}, \\
B_{1n} = -B_{3n} = 1, \quad B_{2n} = -B_{4n} &= \frac{\sinh(\beta_n b) - \sin(\beta_n b)}{\cos(\beta_n b) - \cosh(\beta_n b)}, \\
\alpha_m = \lambda_m/a, \quad \beta_n = \lambda_n/b \quad (m = 1, 2, \dots; n = 1, 2, \dots) & \tag{17}
\end{aligned}$$

The parameters  $\lambda_m$  and  $\lambda_n$  in the two directions are obtained by solving the following equation:

$$\cosh(\lambda) \cos(\lambda) - 1 = 0$$

The 5 first zeros of the previous equation are calculated numerically by a dichotomic algorithm. The solutions are:

$$\begin{aligned}
\lambda_1 &= 4.73004074692726 \\
\lambda_2 &= 7.85320462584495 \\
\lambda_3 &= 10.99560784101484 \\
\lambda_4 &= 14.13716549277302 \\
\lambda_5 &= 17.27875965833661
\end{aligned} \tag{18}$$

and when  $m, n > 5$  the parameters  $\lambda_i$  ( $i = m, n$ ) are accurately approximated by the formula:

$$\lambda_i = \frac{\pi}{2} + i\pi \quad \text{if } i > 5.$$

Then, the wave numbers  $\xi_m$  and  $\eta_n$  come from the Fourier transform in the space domain (6) applied to the mode shape (14):

$$\xi_m = \frac{\alpha_m}{a}, \quad \eta_n = \frac{\alpha_n}{b}$$

When  $m,n > 5$ , the wave numbers in the directions  $x$  and  $y$ , are determined analytically

$$\xi_m = \left(m + \frac{1}{2}\right) \frac{\pi}{a}, \quad \eta_n = \left(n + \frac{1}{2}\right) \frac{\pi}{b} \tag{19}$$

The identification of the bending rigidities of a clamped plate begins with the modal analysis of the structure and the identification of mode shapes that present nodal lines in the directions parallel to the boundaries of the plates. These eigen-modes are identified by a couple of integers ( $m,n$ ) and by an angular frequency denoted by  $\Omega_{mn}$ . Then, the approximated wave numbers ( $\xi_m,\eta_n$ ) associated to the mode shape  $W_{mn}$  of the clamped plate given by formula (19) and the corresponding measured angular frequencies  $\Omega_{mn}$ , are introduced in the inverse problem given by formula (12) and (13). These formula lead to the estimated elastic properties of the plate.

The reader will notice that the numerical effort necessary to perform this identification is very small: it only requires to firstly compute the matrices  $[A]$  and  $[B]$  appearing in expression (12), with the wave numbers  $\xi_m$  and  $\eta_n$  given by formula (19). The solution of system (12) is then performed in a least mean squares sense according to expression (13). Clearly, the main advantage of this identification method is to avoid the problem of explicitly solving the plate equations (1a,1b).

As already mentioned, this system will however be solved in the next sections only in order to provide a numerical validation of this identification method. In fact, the solutions thus obtained will play the role of the “true” displacement fields of the plate for given specially orthotropic plates with well-known elastic properties.

3.3. Numerical test-case

In this section, the method proposed for the evaluation of the elastic constants of a specially orthotropic plate submitted to both simply supported and clamped boundary conditions is analyzed through a numerical experiment. The vibration of the specially orthotropic plate is computed by solving the system (1a,1b) with the high-order finite differences method presented in details in [13]. The eigen-modes and eigen-frequencies coming from this direct problem, are then introduced in the inverse problem presented in the previous section. The structure is a  $0.8 \times 0.8$  carbon/epoxy plate of thickness  $h = 10^{-3}$  m,  $E_1 = 120$  GPa,  $E_2 = 10$  GPa,  $G_{12} = 4.9$  GPa,  $\nu_{12} = 0.3$ ,  $\rho = 1510$  kg/m<sup>3</sup>. This direct problem is solved on a  $36 \times 36$  mesh-grid.

Tables 1 and 2 present the results of the identification of the elastic constants of the test-plate performed successively with the 10 first modes of the plate, from the 10th mode to

Table 1  
Simply supported plate

	Elastic constants (GPa)		
	$E_1$	$E_2$	$G_{12}$
Computed constants	120	10	4.9
Identified constants with modes $1 \rightarrow 10$	119.99	9.998	4.901
Identified constants with modes $10 \rightarrow 20$	119.99	10	4.898
Identified constants with modes $1 \rightarrow 20$	119.99	10	4.898



Table 2  
Clamped plate

	Elastic constants (GPa)		
	$E_1$	$E_2$	$G_{12}$
Computed constants	120	10	4.9
Identified constants with modes 1 $\rightarrow$ 10	115	9.4	3.6
Identified constants with modes 10 $\rightarrow$ 20	118	9.5	3.8
Identified constants with modes 1 $\rightarrow$ 20	125	9.5	3.8

the 20th mode, and finally with the 20 first modes of the plate. In [Tables 1 and 2](#), the measured frequencies are the “true” frequencies given by the vibration calculus as already explained. More precisely, [Table 1](#) refers to a simply supported plate, and [Table 2](#) concerns a clamped plate.

The results of this numerical validation for the simply supported plate are “excellent” since the inverse problem (8), (12) and (13), solves exactly the system (1a,1b).

[Fig. 1](#) shows the 9 first modes of the carbon/epoxy test-plate.

The results of the identification of the elastic constants of our test-plate from measurements on a clamped plate are less satisfactory than those obtained when the identification

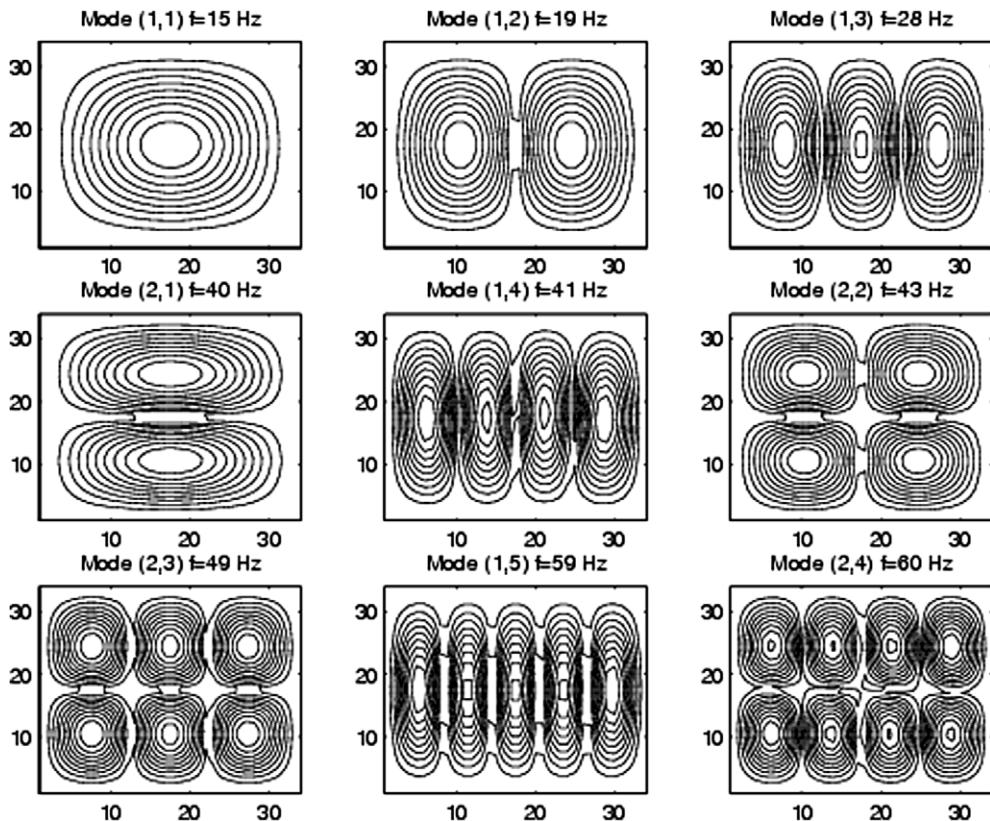


Fig. 1. Modes of the carbon/epoxy clamped test-plate.

is performed on the simply supported plate: the reason lies in formula (14) which only gives approximate values of the wave numbers of the clamped plate. Thus, the resulting wave numbers  $(\xi_n, \eta_n)$  given by (19) are also approximate values.

It was interesting to check the method in the case of disturbed measurements. That is the aim of Tables 3 and 4. A centered 10 Hz random noise has been added to the preceding computed frequencies, in order to model a measurement noise. More precisely, Table 3 presents the exact/disturbed frequencies, and Table 4 presents the elastic moduli identified in presence of this noise.

Table 4 shows that even with this 10 Hz noise which represents an error of 30% on the frequency of the first mode shape of the plate, the identification converges in a satisfactory way to the computed elastic moduli. In all cases, the in-plane shear modulus  $G_{12}$  is not described as well as the transverse moduli  $E_1$  and  $E_2$ . The reason for this lies presumably in the fact that for the structure considered here, namely a carbon–epoxy plate, the shear modulus  $G_{12}$  is 24 times smaller than  $E_1$ , and 2 times smaller than

Table 3  
Frequency noise

	Frequency (Hz)	
	Exact	Perturbed
Mode 1	15.39	10.97
Mode 2	19.65	18.18
Mode 3	28.54	31.67
Mode 4	40.42	35.52
Mode 5	41.97	38.36
Mode 6	43.38	40.41
Mode 7	49.67	46.66
Mode 8	59.57	60.61
Mode 9	60.24	57.96
Mode 10	75.41	72.40
Mode 11	78.41	73.56
Mode 12	85.90	88.37
Mode 13	95.10	94.55
Mode 14	119.09	123.41
Mode 15	123.51	123.17
Mode 16	129.11	128.30
Mode 17	131.44	134.90
Mode 18	142.87	143.12
Mode 19	153.27	150.30
Mode 20	167.61	169.33

Table 4  
Clamped plate and perturbed frequencies

	Elastic constants (GPa)		
	$E_1$	$E_2$	$G_{12}$
Computed constants	120	10	4.9
Identified constants with modes 1 → 10	113	7.2	7.1
Identified constants with modes 10 → 20	123	10	3.5
Identified constants with modes 1 → 20	120	10	2.9

$E_2$ , and therefore, its influence on the response of the structure remains small. In general, identification errors increase with parameters which have a small influence on the response of the system.

In conclusion, the identification of the elastic constants of a specially orthotropic plate presented in this section provides satisfactory results. The method is very simple to implement and fast to run. More precisely, computing an identification sequence requires to inverse a  $3 \times 3$  positive definite matrix: we used a Cholesky method was used in the present article. This method works well at low frequency; i.e., on the first modes of the structure which are easy to measure with an impact testing hammer and an accelerometer, for example.

#### 4. Middle frequency identification: The I.W.C. approach

##### 4.1. Method principle

We first review the method developed in [11]. Based on rather high frequency assumptions, this approach leads to the assessment of a dispersion equation associated with the spatial vibrational field of a plate, denoted  $w$ . The main idea is to project the actual vibrational field on a set of inhomogeneous damped waves parameterized with the parameter triplets  $(k, \theta, \eta)$ , as follows:

$$o_{k,\theta,\eta}(x, y) = e^{-ik((1+i\eta)x \cos \theta + y \sin \theta)} \quad (\text{damped plane waves}) \quad (20)$$

A correlation index between the harmonic field, namely the Fourier transform of the spatial field  $w$ , and each of the preceding parameterized waves  $o$ , called IWC (“inhomogeneous wave correlation”), depending on the wave propagation parameters is computed as follows:

$$\text{IWC}(k, \theta, \eta) = \frac{\left| \int \int_S w o_{k,\theta,\eta}^* dx dy \right|}{\sqrt{\left| \int \int_S |w|^2 dx dy \right| \int \int_S |o_{k,\theta,\eta}|^2 dx dy}} \quad (21)$$

where  $a^*$  denotes the complex conjugate of  $a$ . The reader will notice that the frequency does not appear explicitly in the preceding equations. As a consequence, this method can be classified as a *nonlinear correlation identification method* according to the terminology employed in the control theory literature.

In other words,  $\text{IWC}(k, \theta, \eta)$  represents the “contribution” of the wave  $o$  to the field  $w$ , i.e., the part of the energy supported by this wave of the total energy brought by the field. In the middle and high frequency domains, due to important modal overlapping phenomena, the actual field includes waves in all the directions  $\theta$ . Therefore, the efficiency of this index strongly depends upon the modal overlap of the field  $w$ . The search for a maximum of this correlation index allows us to define a wave in any direction  $\theta_i$  investigated, and thereby to assess the dispersion equation of the plate. Fig. 2 shows a 2D map of the displacements obtained at frequency 560 Hz and the wave numbers  $k$  estimated at this frequency with an angular step of  $\Delta\theta = 5^\circ$ .  $\hat{k}$  (respectively,  $\hat{o}$ ) denotes the estimate of the wave number (respectively, the inhomogeneous wave) given by the maximization of the IWC index.

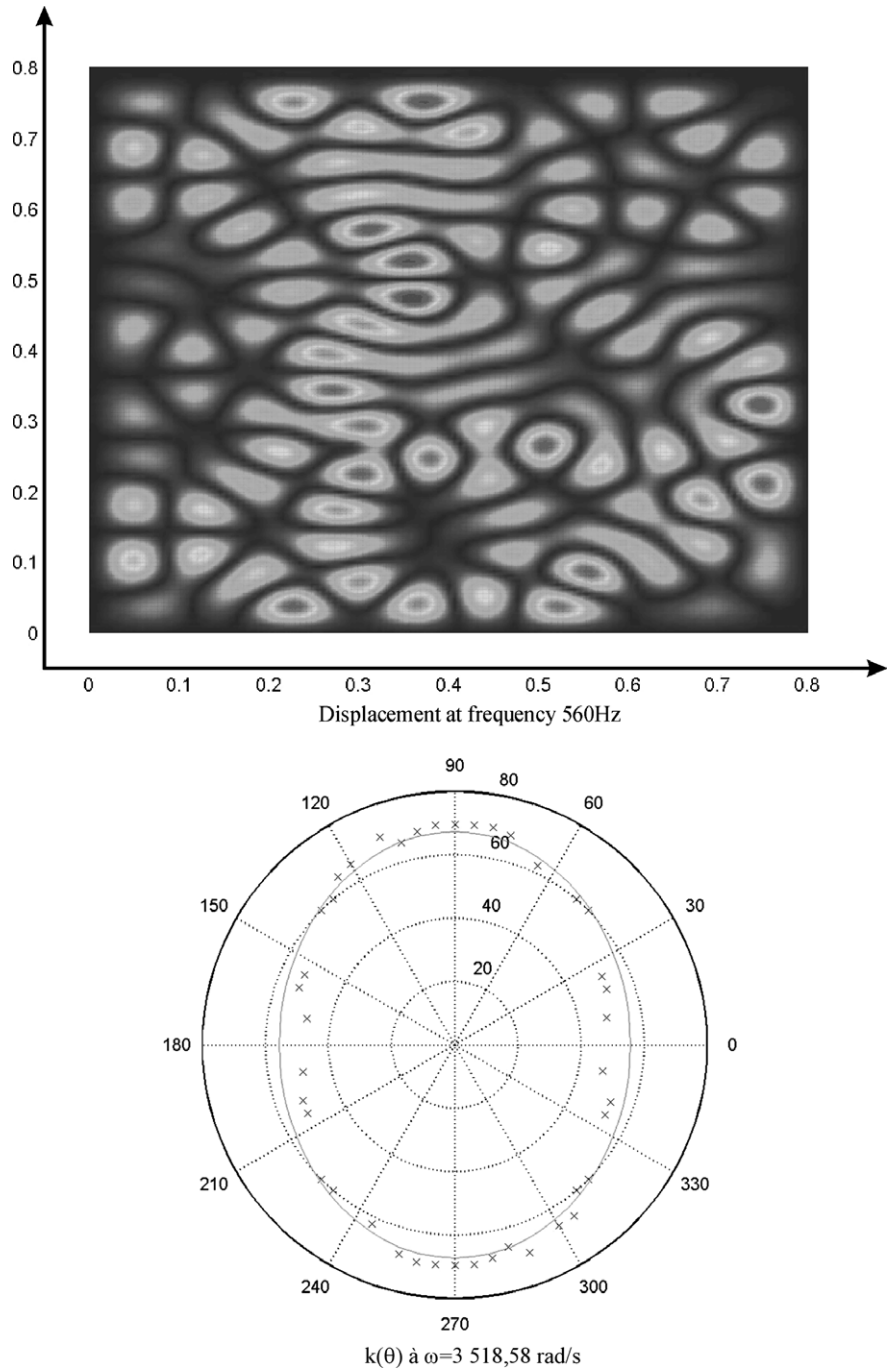


Fig. 2. Identification example at frequency  $f=560\text{ Hz}$ . The angular step is  $\Delta\theta=5^\circ$ : displacement field (up), wavenumbers map (down).

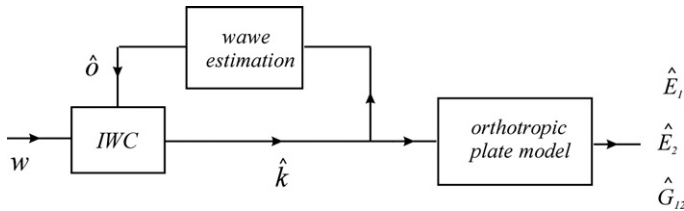


Fig. 3. Plate identification block diagram.

The IWC method implicitly permits to avoid the singular variations of the space field, thus making this approach somehow independent of the boundary conditions and of the signal source. This dispersion equation is then treated in order to provide a model of the equivalent orthotropic plate equivalent to the original one, as shown in Fig. 3.

In order to assess the flexural rigidities of the plate, i.e.,  $(D_1, D_2, D_{12})$ , we refer to the classical formalism of [15]:

$$\sigma\omega^2 = k^4(D_1 \cos^4 \theta + D_2 \sin^4 \theta + D_{12} \cos^2 \theta \sin^2 \theta) \quad (22)$$

The estimates of the flexural rigidities ( $\hat{D}_1, \hat{D}_2$ , and  $\hat{D}_{12}$ ) of the equivalent orthotropic plate, come from the identification of the wave numbers  $k(\theta)$  that maximize the IWC index in Eq. (21), and the minimization of a least squares index based on the formalism of Eq. (22). We therefore derive the mechanical constants, or more precisely their estimates, of the equivalent plate as follows:

$$\hat{E}_1 = \frac{12}{h^3} \hat{D}_1 (1 - \nu^2), \quad \hat{E}_2 = \frac{12}{h^3} \hat{D}_2 (1 - \nu^2), \quad \hat{G}_{12} = \frac{12}{h^3} \hat{D}_1 (0, 5\hat{D}_{12} - \nu\hat{D}_2) \quad (23)$$

#### 4.2. Validation on a numerical experiment

The link between the direct problem and the inverse problem has been used in order to check the properties of the IWC method. The vibratory response of the special orthotropic carbon–epoxy plate, already used in Section 3.3, with dimensions  $800 \times 800 \times 1$  mm excited by a white noise source term is computed according to the model presented in Section 2 above, leading to vibratory velocity (or displacement) maps lying on a  $64 \times 64$  nodes mesh-grid.

We notice that the identification procedure presented above is limited in the frequency domain. The low frequency limitation comes from the constraint that one must work in a domain of strong modal density (remember that one single resonant mode only represents two points in the wave numbers plane while the estimation algorithm is trying to find it in any direction). Moreover, the high frequency limitation comes from the spatial sampling of the structure studied: Shannon's theorem states that it is impossible to identify the wave numbers greater than  $f_s/2$  where  $f_s$  is the inverse of the spatial sampling step. The reader may notice that this plate presents an important structural orthotropy. The main material properties are (see Section 2 for notations):  $E_1 = 120$  GPa,  $E_2 = 10$  GPa,  $G_{12} = 4.9$  GPa,  $\nu_{12} = 0.3$  and  $\rho = 1510$  kg m<sup>-3</sup>.

Let us remember that the harmonic displacement maps are computed by solving system (1a,1b) in the frequency range [100–1800 Hz].

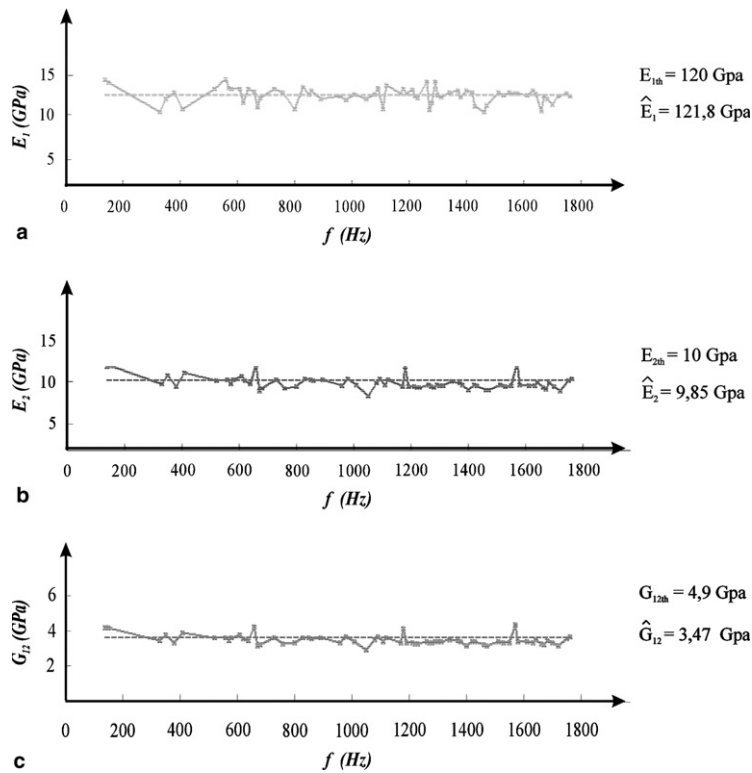


Fig. 4. Elastic constants identification from simulated measures (dot curves: mean values w.r.t. frequency).

Finally, the IWC method is applied at each measured frequency and the elasticity constants are obtained by an averaging procedure upon the intended frequency range, as shown in Fig. 4.

4.3. Comparison with the modal approach

The results obtained by both methods are rather satisfactory. In both cases, one can notice that the shearing factor is underestimated: the error is merely 20%. This can be explained by the fact that the rigidity constant  $G_{12}$  is very small, compared to the value of  $E_1$ , namely 4% of  $E_1$ . Since the identification is based on the global estimation of the three constants  $E_1$ ,  $E_2$  and  $G_{12}$ , the absolute errors made on each of these three constants are similar and comparatively, the relative error made on the estimation of  $G_{12}$  is greater than the one made on the other constants. Complete results are presented in Table 5.

Table 5  
Comparison between modal approach and IWC approach: elastic constants (GPa)

	Elastic constants (GPa)		
	$E_1$	$E_2$	$G_{12}$
Computed constants	120	10	4.9
Modal approach	125	10	3.9
IWC approach	121.8	9.85	3.47

The main interest of the modal approach is its efficiency from the very first modes of the plate and especially in the low frequency domain where their measurements are easily available. Its main drawback is its great sensitivity to the boundary conditions.

The IWC method requires to work at rather high frequencies and needs a lot of data in order to accurately define the vibratory behavior of the structure. Its main advantage is to be almost independent of the boundary conditions and of the nature of the excitation source.

#### 4.4. Application to an experimental case

Our concern is now to apply the preceding identification method to complex structures such as the ones encountered in the helicopter interior trim, in real excitation conditions in flight, as well as in artificial conditions. The harmonic vibratory field is measured by near-field acoustic holography (NAH) techniques. A bi-dimensional network of microphones provides experimental measures used to solve the reverse problem (back-propagation to the source plan phenomenon), i.e., to recover the field on the plane area so analyzed. The interested reader can refer to [16,17] for example. NAH permits the representation of the vibratory velocity fields with a convenient resolution. In fact, the measurement is done in the near-field of the source so the evanescent waves are taken into account in the reconstruction process of pressure and velocity spatial fields.

In practice, the study of stationary phenomena allows us not to measure simultaneously all the network nodes, so a reduced number of microphones have to be moved

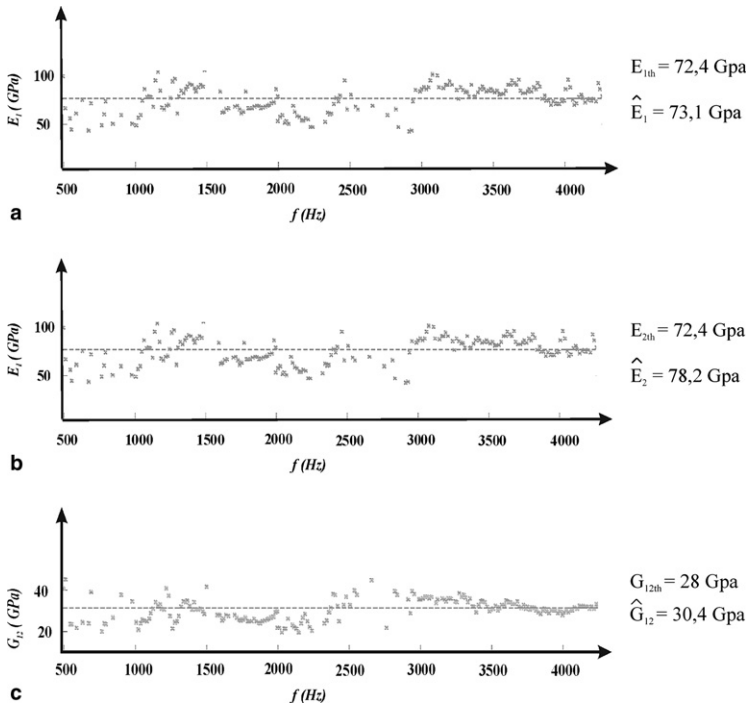


Fig. 5. Parameter identification from experimental measures (dot curves: mean values w.r.t. frequency).

to cover the source area, provided a phase reference is used during the whole measurement campaign (for more details, see for example [18]). Nevertheless, this method presents some limitations and requires rather sophisticated algorithms. Classically, filtering procedures are necessary to avoid problems linked to the amplification of noisy components during the back-propagation process. The reader interested in the algorithms we used, may refer to [19] for example.

In order to justify using acoustic holography techniques in the identification procedure, an experimental setup has been realized, using an homogenous and isotropic aluminium plate with dimensions  $800 \times 800 \times 5$  mm. The mechanical properties of this plate are known “a priori”:  $E_1 = E_2 = 72.4$  GPa,  $G_{12} = 28$  GPa,  $\nu_{12} = 0.3$  and  $\rho = 2770$  kg m<sup>-3</sup>. This plate is excited by a modal shaker providing a white noise acceleration in the frequency range of interest [10;6000 Hz]. The excitation signals are captured by an accelerometer located at the excitation point and the acoustic pressure is measured by an antenna with 64 microphones. A fixed microphone acting as a phase reference, allows us to move the antenna in order to entirely cover the plate surface, thus defining a final network with  $40 \times 40$  nodes leading to the vibration velocity field  $w$  of the IWC approach. Complete identification results are given in Fig. 5.

The dispersion of the results thus obtained is greater than in simulation (see Fig. 5). Nevertheless, they remain quite satisfactory since we consider their mean values with respect to the frequency, and this, despite the difficulties of the measurement procedure and the errors due to the holography method itself.

## 5. Conclusion

In this paper, we presented and discussed two identification methods of the plate elasticity constants based, respectively, on a modal representation and on an ondulatory description of the vibrations. These methods have been validated and compared on a numerical example and an experimental example. Our work shows that we have now at our disposal a complete range of identification tools covering the low frequency domain as well as the high frequency domain. We can now apply these techniques to more complicated structures such as complex panels made of composite materials together with stiffeners. Indeed, these structures will be modelled by plane orthotropic descriptions whose vibratory behavior is predictable under given excitations.

Moreover, these methods allow us to simplify the numerical modelling of complex structures (homogenization problem): finite element representations, statistical energy analysis, ... so as to derive their vibro-acoustic behavior.

As an application, it will be interesting to model complex structures such as an helicopter cabin, in order to derive the inner acoustic radiation and to better control its propagation.

In a forthcoming work, we will investigate the delicate problem of the structural damping estimation which is not yet satisfactorily treated, neither by modal nor correlation approaches.

## References

- [1] Caillet J, Marrot F, Dupont P, Malburet F, Carmona JC. Nearfield acoustic holography measurement inside a helicopter cabin. In: ETTC 2005, International conference on test and telemetry, Toulouse, France, 7–10 June, 2005.



- [2] Aksu G, Ali R. Free vibrations analysis of stiffened plates using finite difference method. *J Sound Vib* 1976;48:15–25.
- [3] Mukhopadhyay M. Vibration and stability analysis of stiffened plates by semi-analytic finite difference method, Part 1: Consideration of bending displacements only. *J Sound Vib* 1989;130:27–39.
- [4] Koto TS, Olson MD. Vibration analysis of stiffened plates by super elements. *J Sound Vib* 1992;158:149–67.
- [5] Ahmadian MT, Sherafati Zangeneh M. Vibration analysis of orthotropic rectangular plates using superelements. *Comp Meth Appl Mech Eng* 2002;191:2069–75.
- [6] Dalaei M, Kerr ADR. Natural vibration analysis of clamped rectangular orthotropic plates. *J Sound Vib* 1996;189:399–406.
- [7] Muthurajan KG, Sanakaranarayanan K, Nageswara B Rao. Evaluation of elastic constants of specially orthotropic plates through vibration testing. *J Sound Vib* 2004;272:413–24. Evaluation of elastic constants of specially orthotropic plates through vibration testing.
- [8] Grédiac M, Vautrin A. Mechanical characterization of anisotropic plates, experiments and results. *Eur J Mech A/Solids* 1993;12:819–38.
- [9] Deobald R, Gibson RF. Determination of elastic constants of orthotropic plates by a modal analysis/ Rayleigh–Ritz technique. *J Sound Vib* 1993;124:169–83.
- [10] Grédiac M, Paris PA. Direct identification of elastic constants of anisotropic plates by modal analysis: theoretical and numerical aspects. *J Sound Vib* 1996;195:401–15.
- [11] Berthaut J, Ichchou Jezequel L. Identification large bande des paramètres équivalents de structures 2-D anisotropes dans l'espace des nombres d'ondes. *Mécanique Industries* 2003;4:377–84.
- [12] Au FTK, Wang MF. Sound radiation from forced vibration of rectangular orthotropic plates under moving loads. *J Sound Vib* 2006;281–3:690–8.
- [13] Mazzoni D. An efficient approximation for the vibro-acoustic response of a turbulent boundary layer excited panel. *J Sound Vib* 2003;264:951–71.
- [14] Leissa AW. Vibration of plates. National Aeronautics and Space Administration, SP 160; 1969.
- [15] Timoshenko S, Woinovsky-Krieger S. Theory of plates and shells. New York: McGraw-Hill; 1959.
- [16] Maynard JD, Williams EG, Lee Y. Nearfield acoustical holography: 1. Theory of generalized holography and the development of NAH. *J Acoust Soc Am* 1985;8:1395–413.
- [17] Hald J. A unique technique for scan-based near-field acoustic holography without restrictions on coherence. *B&K Tech Rev* 1989;1:1–50.
- [18] Pascal JC. Les techniques d'imagerie acoustique et l'holographie acoustique. In: Proceedings of Journée imagerie acoustique appliquée, CRITT-M2A, 5 November; 2002.
- [19] Vaucher-Delacroix D, Chevret P, Perrin F. Use of acoustic holography in 3D interior measurements. In: Proceedings of Internoise, Dearborn, MI, USA, August 19–21; 2002.